P H Y S I C A L   R E V I E W   L E T T E R S

Endotaxial Silicide Nanowires

Zhian He,[1] David J. Smith,[2,3] and P. A. Bennett[3]

[1]*Science and Engineering of Materials Program, Arizona State University, Tempe, Arizona 85287-1504, USA*
[2]*Center for Solid State Science, Arizona State University, Tempe, Arizona 85287-1504, USA*
[3]*Department of Physics and Astronomy, Arizona State University, Tempe, Arizona 85287-1504, USA*

We demonstrate the growth of self-assembled nanowires of cobalt silicide on Si(111), (100), and (110) substrates during deposition of Co onto a heated Si substrate. Silicide islands form via an endotaxial mechanism, growing into the substrate along inclined Si{$\bar{1}11$} planes, which breaks the symmetry of the surface and leads to a long, thin nanowire shape. During growth, both the length and width of the islands increase with time in a fixed proportion that varies strongly with growth temperature, which shows that the nanowire shape is kinetically determined. It is expected that nanowires could form in many other overlayer/substrate systems via this mechanism.

The topic of self-assembled epitaxial nanostructures has been widely studied, beginning with the Ge/Si(100) system, where the concept of "coherent islands" and "quantum dots" originated [1–5]. In these systems, strain is intimately coupled with the shape, size, and spacing of small island structures. In related fashion, it has been found that rare-earth (RE) metals deposited onto heated Si(100) form self-assembled nanowire (NW) structures that are very long and narrow [6–9]. This shape is believed to result from anisotropic lattice mismatch that is small ($\sim$0%) in the long direction and large ($\sim$8%) in the narrow direction of the NW. Such structures have potential applications as low-resistance interconnects, sensors, or nanoscale contacts to quantum dots or molecular structures. Their small size, self-assembled nature, high crystalline quality, and silicon compatibility offer advantages over other types of metallic NWs produced by various methods including chemical vapor deposition (CVD), nanopores, scanning probes, or lithography [10–13].

From a practical viewpoint, rare-earth metals on Si(100) represent a materials system with limited structural, chemical, and electronic properties. In this Letter, we introduce a mechanism that allows NW growth for several transition metal silicides on Si(111), (100), and (110). This mechanism involves epitaxial growth *into* the substrate, hence the name "endotaxy," as originally coined by Fathauer *et al.* [14]. This mechanism does not require anisotropic lattice mismatch; it allows for a variety of metals and substrates and it allows tuning of the NW aspect ratio via the growth temperature.

Si substrates (*p*-type, 1 Ω cm) were prepared by flashing to 1250 °C in ultrahigh vacuum. Cobalt was deposited by sublimation from a high-purity wire onto a heated substrate. Temperature was calibrated with an optical pyrometer. Coverage is stated in monolayer units, where 1 ML = 1 metal atom per 1 $\times$ 1 surface mesh. Samples were quenched immediately after growth, then removed for *ex situ* imaging using a Digital Instruments

Multimode III Atomic Force Microscopy (AFM) in contact mode, and a JEOL 4000EX high-resolution electron microscope (HREM).

Figure 1 shows islands grown on Si(111) at 800 °C. Two distinct shapes occur: equilateral triangles that are approximately 200 nm on each edge and long, narrow NW structures that are approximately 10 nm wide $\times$ 1000 nm long. The cross-section HREM micrographs show that these two island shapes have different structures at their silicide/silicon interface: the triangular islands grow *above the* substrate with a coherent A-type Si(111) interface. The NW islands grow *into* the substrate with a coherent B-type Si(11$\bar{1}$) interface inclined to the
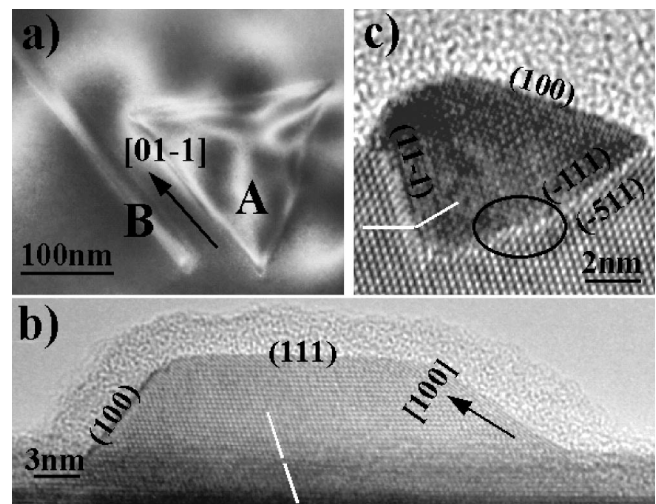

FIG. 1. Islands formed by deposition of 1 ML Co on Si(111) at 800 °C. (a) Plan-view TEM of triangular and nanowire shapes marked A and B, respectively. HREM cross sections along Si[01$\bar{1}$] of triangular island (b) and NW island (c), viewed along its length. The three sides of the triangle are {100} facets. The oval indicates a growth ledge. The broken white lines indicate B-type vs A-type interfaces.

surface on one long edge and $CoSi_2(\bar{1}11)//Si(\bar{5}11)$ along the opposite long edge. The B-type interface refers to a twin boundary, [15] which is readily visible in atomic resolution images as denoted by the kinked white lines in the figure. The $Si(11\bar{1})$ edge has no defects, while the $Si(\bar{5}11)$ edge contains a growth ledge.

Figure 2 shows islands grown on Si(100) at 750 °C. Two distinct shapes occur: rectangles with average lateral dimensions 30×200 nm and NWs with average lateral dimensions 15×500 nm. In the plan-view electron micrograph, the rectangles are bright, while the NWs are dark, suggesting a different crystal type and/or orientation. The cross-section HREM micrographs again show that these two island shapes have different structures at their buried interfaces: the rectangular islands have A-type interfaces, while the NWs have B-type on one side and $CoSi_2(\bar{1}11)//Si(\bar{5}11)$ along the other, exactly as for the NWs on Si(111). The rectangular islands are bounded by $CoSi_2\{100\}$ and $\{111\}$ facets. The NW islands are bounded by $CoSi_2\{111\}$, $\{100\}$, and $\{011\}$ facets. The Si(111) edge is perfect, while the $Si(\bar{5}11)$ edge contains a growth ledge.

Figure 3 shows islands grown on Si(110). Only NW shapes occur, and with a single orientation, along $Si(\bar{1}11)$. For growth at 780 °C, 1 ML/min, 20 sec, the average island dimensions are 35 nm wide by 500 nm long, while at 740 °C, 2 ML/min, 30 sec, the island dimensions are 20 nm wide by 700 nm long. The cross-section

FIG. 2. Islands formed by deposition of 1 ML Co on Si(100) at 750 °C. (a) Plan-view TEM showing rectangular and NW shapes, marked A and B, respectively. HREM cross sections along $Si[01\bar{1}]$ of rectangular (b) and nanowire (c) islands, viewed along their length. The oval indicates a growth ledge. The broken white line indicates B-type vs A-type interface.

HREM micrograph shows that the buried interfaces for these islands are B-type (111) along one edge and $CoSi_2(\bar{1}11)//Si(\bar{5}11)$ along the other, as for the other two substrates.

Figure 4 shows the time dependence of the NW dimensions for Co/Si(110) at 780 °C. We show the length (L), width (W), and aspect ratio (L/W) for three different samples grown for three different total times but the same deposition rate of 1 ML/min. Each value represents an average of ~100 islands taken from several AFM images. The error bars indicate 1 standard deviation in each parameter (L, W, and L/W). We find that both L and W increase with time, but the ratio $L/W \sim 15$ is constant. We infer that the island grows with a fixed proportion of length: width: height, in which case each should scale as $t^{1/3}$. This assumes that total volume increases linearly and that no new islands are nucleated. The data are consistent with this scaling, and clearly not consistent with linear L and constant W, as predicted for the Tersoff or Jesson models [4,5]. Similar measurements for growth at 740 °C yield a ratio $L/W \sim 35$. The qualitative difference in aspect ratio is apparent in Fig. 3. We note that the island size (L or W) varies with deposition time, rate, and temperature, but the shape (L/W) varies only with temperature.

It is remarkable that the NW shape occurs at all for these systems, since the overlayer and substrate lattices are closely matched in type (CaF_2 vs diamond) and size (~0.5% mismatch at the growth temperature). Under these conditions, one would expect to see compact island shapes that follow the symmetry of the substrate. Indeed, we find such shapes together with the elongated NW shape. We offer a general explanation for the latter, although specific features differ for each substrate, which we discuss in turn.

For growth on Si(111), the symmetric islands have a perfect equilateral-triangle shape, reflecting the threefold symmetry of the substrate. The islands grow above the substrate with a Si(111) interface that may be either A-type or B-type. In contrast, the NW islands grow *into* the substrate along inclined $Si\{\bar{1}11\}$ planes, and the buried interface is always B-type on one long edge of the island. This interface breaks the symmetry of the surface and leads to the asymmetric island shape. Since the island and substrate lattices match in type and size, the interface on the opposite long edge is also coherent, although it involves high-index planes: $CoSi_2(\bar{1}11)//Si(\bar{5}11)$. This facet is larger than the B-type $(11\bar{1})$ facet, which implies that it advances more slowly, assuming that the island shape is kinetically determined. It is notable that the interface planes are $\{111\}$ silicide, not $\{111\}$ silicon, implying that the rate-limiting step during growth at the interface is silicide formation rather than silicon consumption [16].

The issue of A- vs B-type interface for silicide overlayers on Si(111) has been studied extensively [15–18].

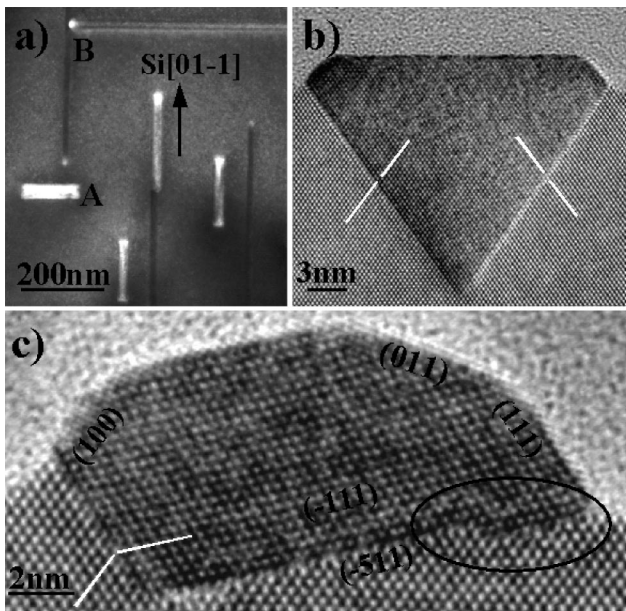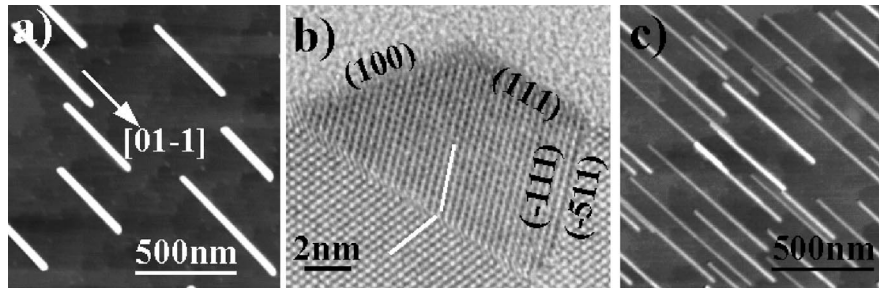FIG. 3.   Islands formed by deposition of Co on Si(110). (a) AFM image for growth at 780 °C, 1 ML/min, 20 sec; (b) HREM cross section along Si[01$\bar{1}$] for islands grown at 700 °C; (c) growth at 740 °C, 2 ML/min, 30 sec.

These interfaces have nearly equal equilibrium energies, but different activation energies for migration [16]. Note that it is geometrically possible to form triangular islands with A-type interfaces along inclined Si{111} planes, but this was not observed. This behavior contrasts with that of bulk precipitates of $CoSi_2$ in Si, where A-type interfaces dominate [19]. Evidently the coupling of interface type with island shape and strain is affected by the elongated shape and partial embedding of the NW islands.

For growth on Si(100), none of the islands grow entirely above the substrate. This would require a Si(100) interface, which is energetically unfavored [20]. All of these islands grow *into* the substrate along inclined Si{$\bar{1}$11} planes. Those islands with A-type interface adopt a rectangular (asymmetric) shape despite the symmetric lattice mismatch. This behavior has been attributed to a strain-driven spontaneous "shape transition" in this system [4,21]. It is not clear whether the genuine NWs occurred and/or were counted in that study. Those islands with a B-type interface form NWs. As for Si(111), the B-type interface breaks the symmetry of the surface and leads to the NW shape. The opposite edge of the NW is also coherent, exactly as for the Si(111) substrate: $CoSi_2(\bar{1}11)//Si(\bar{5}11)$. This face contains a two-layer growth ledge and is longer than the B-type interface, implying that it grows more slowly than the B-type interface.

For growth on Si(110), none of the islands grow entirely above the substrate. This would require a Si(110) interface, which is energetically unfavored. All the islands grow into the substrate along inclined Si{111} planes and all adopt the B-type interface along one edge and a $CoSi_2(\bar{1}11)//Si(\bar{5}11)$ interface on the other. This generates a single island type (all NWs) with a single orientation domain. One small difference compared with Si(111) and Si(100) is that the B-type interface has a larger area than the $CoSi_2(\bar{5}11)$ interface, suggesting that the relative growth rates are inverted (B-type is slower) on Si(110).

Asymmetric island shapes are expected for ingrown islands on each of the three substrates due to the broken symmetry associated with the inclined B-type Si(11$\bar{1}$) interfaces, but it is not obvious why the NWs attain such a dramatic length/width aspect ratio. The kinetic data in Fig. 4 show that the L/W ratio remains constant during growth of the NW: the width simply increases in proportion to the length. This clearly demonstrates that the NW shape is not determined by a strain-driven energetic mechanism, as in the Tersoff or Jesson models, [4,5] since that would imply a maximum or well-defined width. It might be argued that the islands display an equilibrium crystal shape (ECS) that reflects the relative interface energies of the sides vs ends. This hypothesis can be dismissed, however, for several reasons: the NW shape anisotropy (L/W ratio) is much larger than expected for ECS, and specifically for $CoSi_2$ precipitates in Si [19,20]. The system is not in equilibrium, since negligible coarsening occurs at 800 °C [19]; the L/W ratio varies strongly with growth temperature, which is not consistent with a negligible entropy term in the free energy of coherent interfaces [20].

We conclude that the large L/W aspect ratio of the NW shape is kinetically determined: that is, the end vs side facets grow at different rates. These interfaces are crystallographically distinct due to the inclined habit plane, and are expected to have different kinetic behavior. Thus,
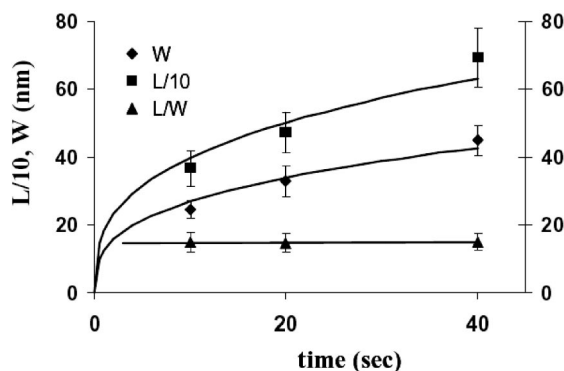

FIG. 4.   Length (L), width (W), and aspect ratio (L/W) vs deposition time for three different Co/Si(110) samples grown at 780 °C and deposition rate 1 ML/min. Error bars represent 1 standard deviation of ~100 islands. Lines show $t^{1/3}$ scaling for L, W, and constant scaling for L/W.

the endotaxial NWs seem to be a surface analog of Widmanstatten precipitates [20]. In such structures, a needlelike shape results from rapid growth at incoherent interfaces at the ends of the needle and slow growth (by ledge mechanism) at coherent interfaces along the sides. It is apparent from our TEM images that the NWs have coherent interfaces along their sides, but the structure at the ends remain unknown. The fact that the L/W aspect varies strongly with growth temperature implies independent thermally activated processes at the end vs sides of the NW. We do not know at present whether the growth rate at each interface is determined by nucleation, diffusion, or attachment kinetics. Jesson *et al.* have pointed out that growth anisotropy can also occur for equivalent interfaces, due to strain effects [5]. Systematic growth studies of individual NWs using an *in situ* imaging probe such as LEEM or TEM would clarify this issue, as we have shown for the Ti/Si(111) system [22].

The endotaxial growth mechanism we have demonstrated here for Co on Si is expected to apply to other systems as well. There are two main requirements. First, the NW material should have a reasonable epitaxial match on some inclined plane. We note that NW growth for $CoSi_2$ on Si(100) or Si(111) requires a B-type interface to break the symmetry, which limits the materials systems. Endotaxial NW growth on Si(110), however, is possible for A-type, or B-type or hexagonal interfaces, which opens further possibilities. Indeed, we have earlier reported NW formation in the Dy/Si(110) system, although the general mechanism and kinetic behavior was not known at that time [23]. Second, significant ingrowth must occur. This may reasonably be predicted from bulk solubility. In this context, we note that NWs form for Ti/Si(111), [22,24,25] even though the crystallographic match is poor, and the solubility is very low. This indicates that the above criteria for endotaxial NW growth are relatively flexible, and suggests that other systems, beyond silicide/silicon, may form NWs by the same mechanism.

[1] C. Teichert, Phys. Rep. **365**, 335 (2002).
[2] D. J. Eaglesham and M. Cerullo, Phys. Rev. Lett. **64**, 1943 (1990).
[3] R. M. Tromp and J. B. Hannon, Surf. Rev. Lett. **9**, 1565 (2002).
[4] J. Tersoff and R. M. Tromp, Phys. Rev. Lett. **70**, 2782 (1993).
[5] D. E. Jesson, G. Chen, K. M. Chen, and S. J. Pennycook, Phys. Rev. Lett. **80**, 5156 (1998).
[6] Y. Chen, D. A. A. Ohlberg, and R. S. Williams, J. Appl. Phys. **91**, 3213 (2002).
[7] J. Nogami, B. Z. Liu, M. V. Katkov, C. Ohbuchi, and N. O. Birge, Phys. Rev. B **63**, 233305 (2001).
[8] B. Z. Liu and J. Nogami, J. Appl. Phys. **93**, 593 (2003).
[9] C. Preinesberger, S. K. Becker, S. Vandre, T. Kalka, and M. Dahne, J. Appl. Phys. **91**, 1695 (2002).
[10] E. S. Snow, P. M. Campbell, M. Twigg, and F. K. Perkins, Appl. Phys. Lett. **79**, 1109 (2001).
[11] A. J. Yin, J. Li, W. Jian, A. J. Bennett, and J. M. Xu, Appl. Phys. Lett. **79**, 1039 (2001).
[12] D. Natelson, R. L. Willett, K. W. West, and L. N. Pfeiffer, Appl. Phys. Lett. **77**, 1991 (2000).
[13] S. M. Prokes and K. L. Wang, Mater. Res. Bull. **24**, 19 (1999).
[14] T. George and R. W. Fathauer, Appl. Phys. Lett. **59**, 3249 (1991).
[15] R. T. Tung, Mater. Chem. Phys. **32**, 107 (1992).
[16] D. Hesse and R. Mattheis, Phys. Status Solidi (a) **116**, 67 (1989).
[17] P. A. Bennett, J. R. Butler, and X. Tong, Jour. Vac. Sci. Technol. A **7**, 2174 (1989).
[18] P. A. Bennett, M. Y. Lee, P. Yang, R. Schuster, P. J. Eng, and I. K. Robinson, Phys. Rev. Lett. **75**, 2726 (1995).
[19] S. Mantl, Mater. Sci. Rep. **8**, 1 (1992).
[20] D. A. Porter and K. E. Easterling, *Phase Transformations in Metals and Alloys* (Van Nostrand Reinhold, New York, 1988).
[21] S. H. Brongersma, M. R. Castell, D. D. Perovic, and M. Zinke Allmang, Phys. Rev. Lett. **80**, 3795 (1998).
[22] P. A. Bennett, B. Ashcroft, Z. He, and R. M. Tromp, Jour. Vac. Sci. Technol. **B20**, 2500 (2002).
[23] Z. He, M. Stevens, D. J. Smith, and P. A. Bennett, Appl. Phys. Lett. **83**, 5292 (2003).
[24] M. Stevens, Z. He, D. J. Smith, and P. A. Bennett, J. Appl. Phys. **93**, 5670 (2003).
[25] Z. He, M. Stevens, D. J. Smith, and P. A. Bennett, Surf. Sci. **524**, 148 (2003).